**[Review Paper]**

# Development of Visible Light Sensitive $TiO_2$ Photocatalysts and Their Sensitization Using $Fe^{3+}$ Ions

Teruhisa OHNO*

Dept. of Materials Science, Faculty of Engineering, Kyushu Institute of Technology,
1-1 Sensui-cho, Tobata-ku, Kitakyushu 804-8550, JAPAN

(Received February 10, 2006)

Titanium dioxide photocatalysts are promising substrates for photodegradation of pollutants in water and air, but show photocatalytic activities only under UV light. To utilize a wider range of incident wavelengths such as solar light, development of photocatalysts active under visible light is very important. Chemically modified titanium dioxide photocatalysts were prepared containing anatase phase with S ($S^{4+}$) substituted for some lattice Ti atoms or N substituted for some lattice O atoms. These catalysts showed strong absorption of visible light and high activities for degradation of 2-propanol in aqueous solution and partial oxidation of adamantane under irradiation at wavelengths longer than 440 nm. The oxidation states of the S and N atoms incorporated into the $TiO_2$ particles were determined to be mainly $S^{4+}$ and $N^{3-}$ from XPS spectra, respectively. The photocatalytic activities of S- or N-doped $TiO_2$ photocatalysts with adsorbed $Fe^{3+}$ ions were markedly improved for oxidation of 2-propanol compared to those of S- or N-doped $TiO_2$ without $Fe^{3+}$ ions under a wide range of incident wavelengths, including UV light and visible light. The photocatalytic activity reached maximum with 0.90 wt% $Fe^{3+}$ ions adsorbed on S-doped $TiO_2$, and 0.36 wt% $Fe^{3+}$ ions on N-doped $TiO_2$. Furthermore, redox treatment of S- or N-doped $TiO_2$ photocatalysts with adsorbed $Fe^{3+}$ ions by reduction with $NaBH_4$ followed by air oxidation resulted in further improvements in photocatalytic activities. In this case, the optimum amounts of $Fe^{3+}$ were 2.81 and 0.88 wt% on the surfaces of S- and N-doped $TiO_2$ photocatalysts, respectively.

**Keywords**

Photocatalyst, Titanium dioxide, Visible light, Sulfur-doped titanium dioxide, Nitrogen-doped titanium dioxide, Iron (III) cation

## 1. Introduction

The discovery of photoelectrochemical splitting of water on titanium dioxide ($TiO_2$) electrodes[1] has lead to many investigations of semiconductor-based photocatalysis[2)~15)]. $TiO_2$ is one of the most promising photocatalysts, and is now used in various practical applications[2),10)], but converts only a small UV band of solar light, about 2-3%, because of its large band gap of 3.2 eV. Therefore, the development of a more efficient $TiO_2$ photocatalyst with a higher photoelectric conversion of visible light is needed. Doping of $TiO_2$ with transition metals[14)~17)] reduced forms of $TiO_x$ photocatalysts[18),19)], and treatment of $TiO_2$ powder with hydrogen peroxide[20)] or chelating agents[21)] have all been investigated, but most of these catalysts do not have long-term stability or sufficiently high activities for a wide range of applications.

N, S, or C anion-doped $TiO_2$ photocatalysts with an anatase structure show a relatively high level of activity when irradiated by visible light[22)~27)]. Recently, we prepared S or C cation-doped $TiO_2$ with an anatase phase and S and C cation-codoped $TiO_2$ with a rutile phase[28)~31)]. However, the photocatalytic activities under visible light irradiation were not sufficient for practical applications. Therefore, we modified these S- and N-doped $TiO_2$ photocatalysts to improve the photocatalytic activities, and developed S-cation doped $TiO_2$[28)~31)].

Here, we report the development of S- and N-doped $TiO_2$ powders and S- and N-doped $TiO_2$ photocatalysts with adsorbed $Fe^{3+}$ ions.

## 2. Experimental

### 2. 1. Materials and Instruments

Various titanium dioxide ($TiO_2$) powders with anatase and rutile crystal structures were obtained from Ishihara Sangyo Kaisha, Ltd. (ST-01, ST-41), Nippon Aerosil Co., Ltd. (P-25) and Toho Titaniumu Co., Ltd. (NS-51). The anatase contents and the surface areas of these powders were as follows: ST-01: 100%,

* E-mail: tohno@che.kyutech.ac.jp

320.5 $m^2/g$; ST-41: 100%, 8.2 $m^2/g$; P-25: 70.0%, 42.5 $m^2/g$; NS-51: 1.0%, 6.5 $m^2/g$. Other chemicals were obtained from commercial sources as guaranteed reagents and were used without further purification. The crystal structures of the $TiO_2$ powders were determined from X-ray diffraction (XRD) patterns. The relative surface areas of the powders were determined with a surface area analyzer. The absorption and diffuse reflection spectra were measured using a spectrophotometer. X-Ray photoelectron spectra (XPS) of the $TiO_2$ powders were measured using a photoelectron spectrometer. Electron spin resonance (ESR) spectra were obtained on a X-band spectrometer.

### 2. 2. Preparation of S- or N-doped $TiO_2$ Powders with Adsorbed $Fe^{3+}$ Ions

S- or N-doped $TiO_2$ powders were synthesized by previously reported methods[28)~31),37)]. To synthesize the S-doped $TiO_2$ powder, titanium dioxide fine powder with anatase phase was mixed with thiourea at a molar ratio of 1 to 1. This mixed powder was calcined at various temperatures under aerated conditions. After calcination, the powder was washed with distilled water and $NH_3$ aqueous solution several times until the pH of the filtrate had become neutral. Urea was used as a doping compound instead of thiourea for preparation of N-doped $TiO_2$. The other experimental conditions were exactly the same as for S-doped $TiO_2$. An appropriate amount of $FeCl_3$ was dissolved in deionized water. The doped $TiO_2$ powder was suspended in an $FeCl_3$ aqueous solution, and the solution was stirred for 2 h. After filtration of the solution, the residue was washed with deionized water several times until the pH of the filtrate became neutral. The powders were dried under reduced pressure at 60°C for 12 h.

### 2. 3. Reduction and Air Oxidation of S- or N-doped $TiO_2$ Powders with Adsorbed $Fe^{3+}$ Ions

S- or N-doped $TiO_2$ powder with adsorbed $Fe^{3+}$ ions was suspended in deionized water. $NaBH_4$ was added to the solution. The solution was stirred for 2 h under aerated conditions. After filtration, the residue was washed with deionized water several times until the pH of the filtrate became neutral. The powders were dried under reduced pressure at 60°C for 12 h.

### 2. 4. Oxidation States of Fe Ions during Photoirradiation under Anaerobic or Aerobic Conditions

ESR spectra of the $Fe^{3+}$ ions adsorbed on the surfaces of the doped $TiO_2$ particles were obtained under reduced pressure at 77 K. A 350-W high-pressure mercury lamp was used as the irradiation light source. The changes in the oxidation condition of Fe ions on doped $TiO_2$ was followed during photoirradiation under reduced pressure.

### 2. 5. Photocatalytic oxidation of 2-propanol on $TiO_2$ powder

Photocatalytic reactions were carried out in a Pyrex tube containing doped $TiO_2$ particles and acetonitrile solution of 2-propanol under aerated condition. S- or N-doped $TiO_2$ photocatalysts with or without adsorbed $Fe^{3+}$ ions or pure $TiO_2$ powder (ST-01) were used as photocatalysts. The suspension was photoirradiated using a 500-W Xe lamp, which emits both UV and visible light over a wide wavelength with an integrated photon flux of $1.1 \times 10^{-2}$ einsteins (E) $s^{-1} \cdot cm^{-2}$ between 350 and 540 nm. To limit the irradiation wavelengths, the light beam was passed through a UV-34, L-42, Y-44, Y-50 or Y-54 filter (Kenko Co.) to cut off wavelengths shorter than 340, 420, 440, 500 or 540 nm, respectively. The amounts of acetone produced by the photocatalytic reactions were determined with a capillary gas chromatograph.

### 2. 6. Photocatalytic Oxidation of Adamantane on $TiO_2$ Powder

A mixture of butyronitrile and acetonitrile was used as the solvent for the reaction because of the low solubility of adamantane in acetonitrile. Photocatalytic reactions were typically carried out in Pyrex glass tubes, to which a mixture of acetonitrile, butyronitrile, adamantane, and $TiO_2$ powder was added under aerated condition. During the reaction, the solution was magnetically stirred and externally photoirradiated. The light source and the method of choosing the incident light wavelength were the same as those used for the photocatalytic degradation of 2-propanol. After photoirradiation for certain time periods, the solution was analyzed with a capillary gas chromatograph.

### 2. 7. Band Calculation

The electronic structures of the S-doped $TiO_2$ were examined using first-principle band calculations to clarify the S-doping effect. The band calculations were carried out by the F-LAPW method[32)] based on the density functional theory[33)] within the generalized gradient approximation[34)]. The calculation methods have been described in detail in previous reports[35),36)].

## 3. Results and Discussion

### 3. 1. Physical Properties of S- and N-doped $TiO_2$ Powders

**Figure 1** shows absorption spectra of S- and N-doped $TiO_2$ photocatalysts, with examples of diffuse reflectance spectra of these powders, together with those of pure rutile and anatase powders. The photoabsorption in the visible region was stronger for S-doped $TiO_2$ powders than for N-doped $TiO_2$ powders[14)]. The relative surface areas of S- and N-doped $TiO_2$ photocatalysts calcined at 500°C were 88.8 $m^2/g$ and 62.2 $m^2/g$, respectively.

### 3. 2. Identification of Chemical States of S Atoms in $TiO_2$ Particles

The chemical states of S and N atoms incorporated into $TiO_2$ were studied by measuring the XPS spectra

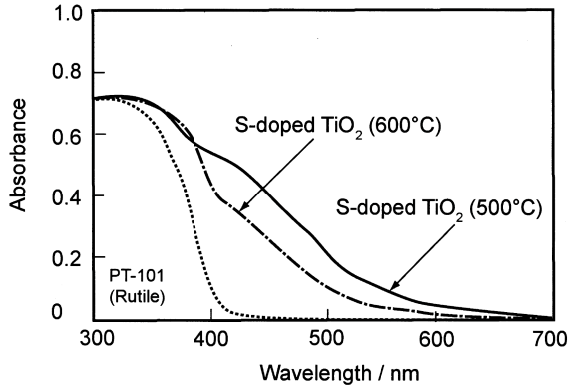


Fig. 1 Diffuse Reflectance Spectra of S-doped and Pure $TiO_2$ Powders (PT-101: rutile)

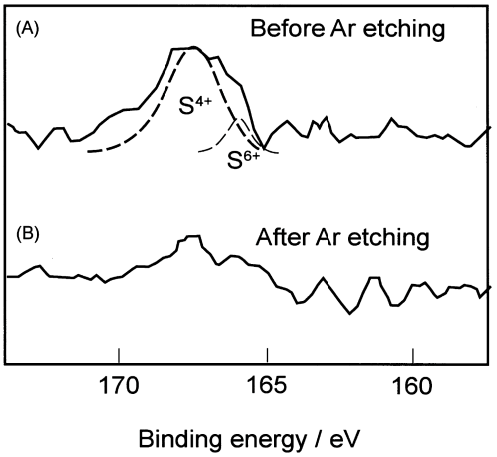


A: After calcination at 500°C and washing with distilled water for 1 h, B: After $Ar^+$ etching.

Fig. 2 XPS Spectra of S-doped $TiO_2$ Powder

of the S- and N-doped $TiO_2$ photocatalysts. After the freshly-prepared S-doped $TiO_2$ powder was washed with deionized water and HCl aqueous solution several times, a weak peak attributable to $S^{4+}$ ion[35),36)] was observed. The peak was also observed after $Ar^+$ ion etching of the sample as shown in **Fig. 2**. The atomic content of S atoms on the surfaces of the S-doped particles was about 1.6% after the washing treatment. The concentration of $S^{4+}$ decreased gradually with depth from the surface of $TiO_2$ to about 0.5% in the bulk. After the freshly prepared N-doped $TiO_2$ powder was washed, a weak peak assigned to $N^{3-}$ (Ti–N) was observed at 396.5 eV. The atomic content of S atoms on the surfaces of the S-doped particles was about 0.9% after the washing treatment[37)].

### 3. 3. Electronic Structures of S-doped $TiO_2$

To determine the effects of doping on the electronic and optical properties of $TiO_2$, the band structures of S-doped $TiO_2$ were analyzed by first-principle band calculations using the super-cell approach. Based on the

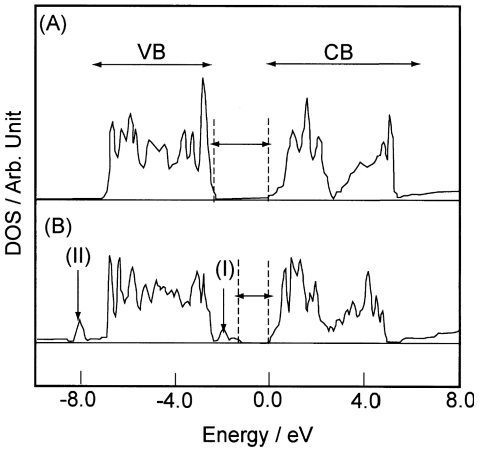


Fig. 3 Total DOS of (A) Undoped and (B) S-doped $TiO_2$

experimental results, the super cell model, in which one S atom is replaced by one Ti atom, contains eight formula units. The density of states (DOS) of undoped $TiO_2$ and S-doped $TiO_2$ are shown in **Fig. 3**. In the undoped $TiO_2$ crystal, the valence band (VB) and conduction band (CB) consist of both Ti 3d and O 2p orbitals. Since the Ti 3d orbital is split into the $t_{2g}$ and $e_g$ states, the CB is divided into lower and upper parts. When $TiO_2$ is doped with S, an electron-occupied level appears above (I) and below (II) the VB. The S 3p states also contribute to the formation of a CB with O 2p and Ti 3d states. The electron occupied level (I) above the VB, which consists of S 3s states, should be important in the photoresponse of $TiO_2$. Electron transition between this level and the VB should be induced by visible light irradiation. This process can explain the findings of visible-light absorption in S-doped $TiO_2$.

### 3. 4. Absorption Spectra of S- or N-doped $TiO_2$ with Adsorbed $Fe^{3+}$ Ions

**Figure 4 (A)** shows absorption spectra of N-doped $TiO_2$ with adsorbed $Fe^{3+}$ ions. The absorption spectra did not change if the amount of $Fe^{3+}$ ions adsorbed on the doped $TiO_2$ was lower than 0.36 wt%. The absorbance of N-doped $TiO_2$ with an amount of $Fe^{3+}$ ions greater than 0.88 wt% increased in the visible light region because Fe compounds are thought to show absorbance in the visible light region. After treatment with $NaBH_4$, the absorbance of N-doped $TiO_2$ with Fe ions in the visible light region increased slightly as shown in **Fig. 4 (B)**. The main factors accounting for these changes are under investigation.

**Figure 5 (A)** shows absorption spectra of S-doped $TiO_2$ with $Fe^{3+}$ ions. The spectra of S-doped $TiO_2$ with adsorbed $Fe^{3+}$ ions in the visible light region depended on the amount of $Fe^{3+}$ ions. No change was observed if the amount of $Fe^{3+}$ ions was less than 0.37 wt%. The absorbance of S-doped $TiO_2$ increased in the visible light region when the amount of $Fe^{3+}$ ions was greater

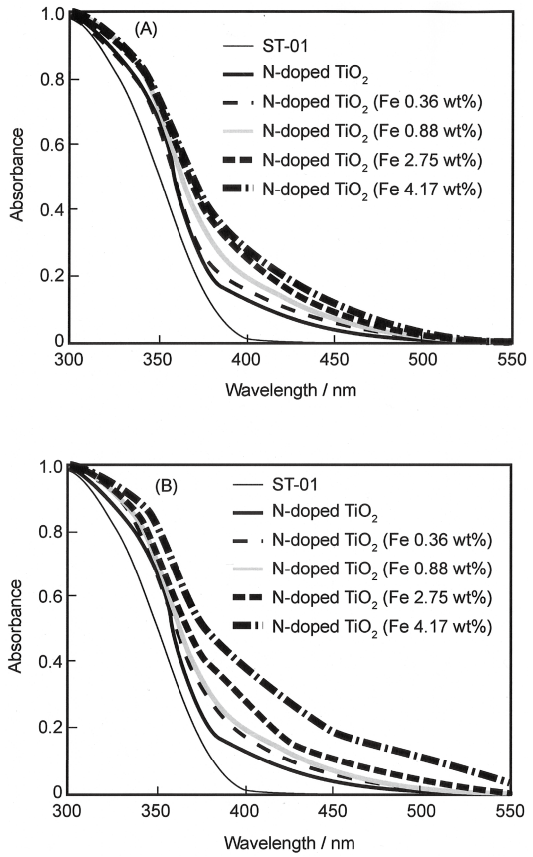


A: Before treatment with $NaBH_4$, B: After treatment with $NaBH_4$ and air oxidation.

Fig. 4 Absorption Spectra of N-doped $TiO_2$ with Adsorbed $Fe^{3+}$ Ions before and after Reduction with $NaBH_4$ Followed by Air Oxidation

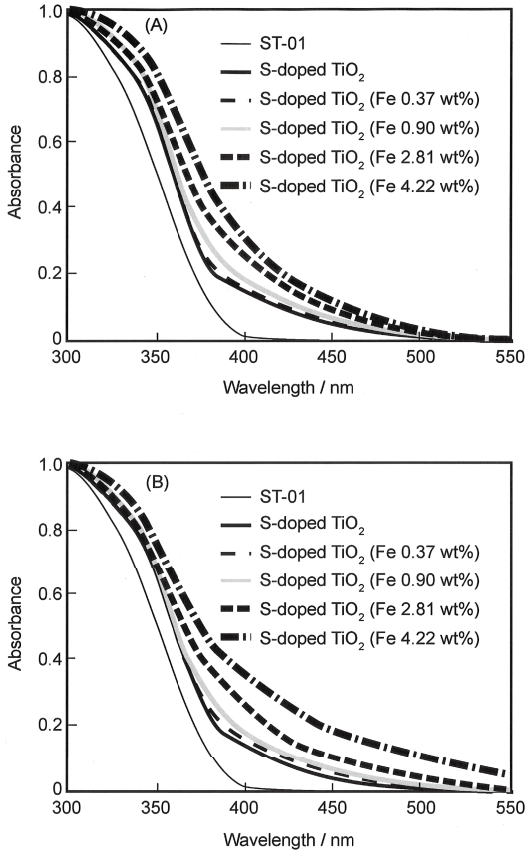


A: Before treatment with $NaBH_4$, B: After treatment with $NaBH_4$ and air oxidation.

Fig. 5 Absorption Spectra of S-doped $TiO_2$ with Adsorbed $Fe^{3+}$ Ions before and after Reduction with $NaBH_4$ Followed by Air Oxidation

than 0.90 wt%. After treatment with $NaBH_4$, the change in the absorbance of S-doped $TiO_2$ with Fe ions in the visible light region was similar to that for N-doped $TiO_2$ with Fe ions (**Fig. 5 (B)**).

### 3. 5. ESR Spectra of S- or N-doped $TiO_2$ with Adsorbed $Fe^{3+}$ Ions under Photoirradiation

**Figure 6** shows ESR spectra of N-doped $TiO_2$ with adsorbed $Fe^{3+}$ ions (0.36 wt%) under irradiation at reduced pressure. A broad peak at 4.4 assigned to the $Fe^{3+}$ species was observed. Under photoirradiation using a high-pressure mercury lamp (350 W; 18.5 mW/$cm^2$) for 5 min, the intensity of the peak assigned to $Fe^{3+}$ was reduced by half as shown in **Fig. 6**. The peak disappeared completely under photoirradiation for more than 20 min. These results suggest that $Fe^{3+}$ ions were efficiently reduced to $Fe^{2+}$ ions that are not detected by ESR measurement, by trapping electrons generated during photoirradiation under reduced pressure. In addition, the peak assigned to $Fe^{3+}$ ions was not changed during photoirradiation under aerated conditions. This result suggests that the rate of generation of $Fe^{2+}$ ions during photoirradiation is much slower than that of the oxidation of $Fe^{2+}$ ions by oxygen.

ESR measurements for S-doped $TiO_2$ with adsorbed $Fe^{3+}$ ions were similar to those for N-doped $TiO_2$ with $Fe^{3+}$ ions. Under reduced pressure, the peak attributed to $Fe^{3+}$ ions decreased because photogenerated electrons were trapped by $Fe^{3+}$ ions on the surface of S-doped $TiO_2$. On the other hand, no change was observed during photoirradiation under aerated conditions.

These results suggest that charge separation between electrons and holes generated photocatalytically was improved because the photoexcited electrons were efficiently trapped by oxygen through $Fe^{3+}$ ions adsorbed on the surface of the doped $TiO_2$ photocatalysts.

Changes in the ESR spectra of S- or N-doped $TiO_2$ with adsorbed $Fe^{3+}$ ions treated with $NaBH_4$ and air oxidation were similar to those of S- or N-doped $TiO_2$ with adsorbed $Fe^{3+}$ ions without treatment.

### 3. 6. XRD Spectra of S- or N-doped $TiO_2$ with Adsorbed $Fe^{3+}$ Ions under Photoirradiation

**Figure 7** shows XRD spectra of N-doped $TiO_2$ with adsorbed $Fe^{3+}$ (4.17 wt%) ions before and after redox

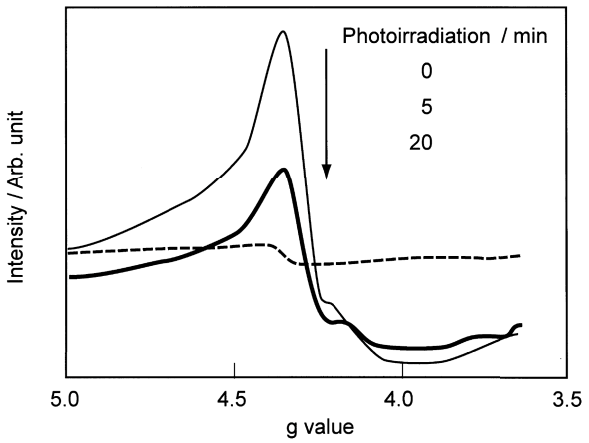


A: Under reduced pressure, B: Under aerated conditions.

Fig. 6 ESR Spectra of N-doped $TiO_2$ with Adsorbed $Fe^{3+}$ Ions (0.36 wt%) before and after Photoirradiation

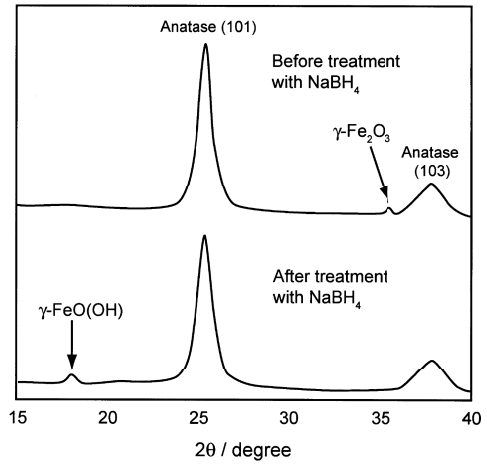


Fig. 7 XRD Spectra of N-doped $TiO_2$ with Adsorbed $Fe^{3+}$ Ions (4.17 wt%) before and after Reduction by $NaBH_4$ Followed by Air Oxidation

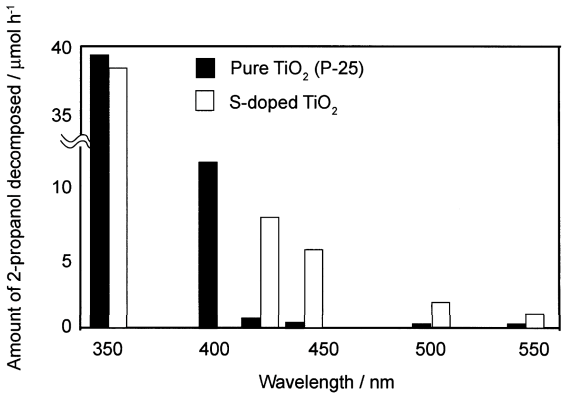


Fig. 8 Photocatalytic Decomposition of 2-Propanol Using S-doped $TiO_2$ or Pure $TiO_2$ (P-25) as a Function of the Cutoff Wavelength for Irradiation from a 1000 W Xe Lamp

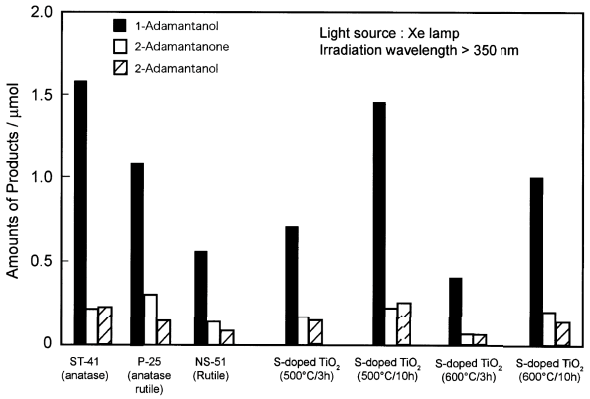


Fig. 9 Amounts of 1-Adamantanol, 2-Adamantanone and 2-Adamantanol Produced from Adamantane after Photoirradiation for 1 h Using Several $TiO_2$ and S-doped $TiO_2$ Catalysts under Photoirradiation at Wavelengths Longer than 350 nm

treatment with $NaBH_4$ under aerated conditions. Before treatment with $NaBH_4$, a small peak was observed at 35.8° assigned to $\gamma$-$Fe_2O_3$. After treatment with $NaBH_4$, a peak appeared at 18.3° assigned to $\gamma$-FeO(OH), and the phase of $\gamma$-$Fe_2O_3$ completely disappeared as shown in **Fig. 7**[38)~40)]. A change in the crystal structure of the Fe compounds on the surface of the S-doped $TiO_2$ particles was also observed before and after redox treatment. As discussed later, the photocatalytic activities of the S- or N-doped $TiO_2$ with adsorbed $Fe^{3+}$ ions are related to the crystal structure of the Fe compounds on the doped $TiO_2$.

### 3. 7. Photocatalytic Activity of S-doped $TiO_2$ Powder for the Decomposition of 2-Propanol

The photodecomposition of 2-propanol was evaluated over pure $TiO_2$ (Degussa, P-25) and S-doped $TiO_2$ (calcined at 500°C for 3 h) powders. **Figure 8** shows the decomposition rate of 2-propanol as a function of the cutoff wavelengths of the glass filters under Xe light. The pure $TiO_2$ powder had similar photocatalytic activity for the photodecomposition of 2-propanol to S-doped $TiO_2$ powders under UV light, but S-doped $TiO_2$ powder showed a much higher level of activity than pure $TiO_2$ powder under photoirradiation at wavelengths longer than 420 nm.

### 3. 8. Photocatalytic Synthesis of Hydroxylated Adamantane Compounds on $TiO_2$

Photocatalytic activities of various $TiO_2$ powders under UV light irradiation were investigated, as shown in **Fig. 9**. 1-Adamantanol, 2-adamantanol, and 2-adamantanone were the main products using all $TiO_2$ powders. Among the pure $TiO_2$ powders, ST-41 powder showed the highest activity. S-doped $TiO_2$ powder calcined at 500°C for 10 h showed activity similar to that of ST-41. The total quantum efficiencies for the pro-

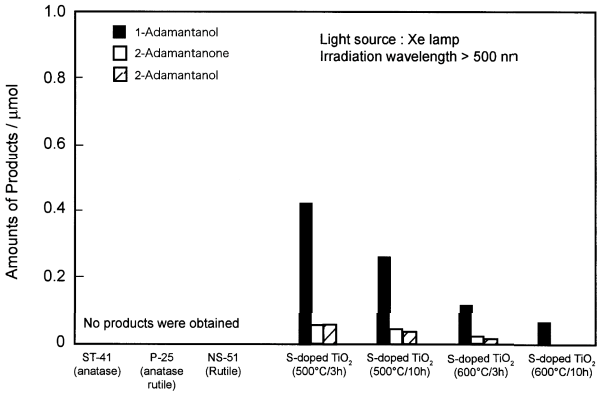


Fig. 10 Amounts of 1-Adamantanol, 2-Adamantanone and 2-Adamantanol Produced from Adamantane after Photoirradiation for 1 h Using Several $TiO_2$ and S-doped $TiO_2$ Catalysts under Photoirradiation at Wavelengths Longer than 500 nm

duction of 1-adamantanol, 2-adamantanol and 2-adamantanone using ST-41 and S-doped $TiO_2$ powder were about 10% and 8.7%, respectively. The activity of S-doped $TiO_2$ under UV light was relatively high compared to that of pure $TiO_2$ photocatalysts.

The photocatalytic activities of S-doped $TiO_2$ powders and pure $TiO_2$ powders were evaluated under visible light at wavelengths longer than 500 nm as shown in **Fig. 10**. S-doped $TiO_2$ calcined at 400°C for 3 h showed the highest activity among the S-doped $TiO_2$ powders examined. On the other hand, no photocatalytic activity was observed with any of the pure $TiO_2$ powders.

### 3. 9. Photocatalytic Oxidation of 2-Propanol

#### 3. 9. 1. Photocatalytic Activities of S- or N-doped $TiO_2$ with Adsorbed $Fe^{3+}$ Ions

**Figure 11 (A)** shows the photocatalytic oxidation of 2-propanol using N-doped $TiO_2$ with various amounts of adsorbed $Fe^{3+}$ ions. ST-01 with anatase fine particles was used as a reference. The photocatalytic activity of N-doped $TiO_2$ increased with higher amount of Fe ions. N-doped $TiO_2$ powders with 0.36 wt% adsorbed $Fe^{3+}$ ions showed the highest activity for oxidation of 2-propanol. As described above, $Fe^{3+}$ ions adsorbed on N-doped $TiO_2$ efficiently trapped the photoexcited electrons, which resulted in improvement of the charge separation between electrons and holes. Above 0.36 wt%, the activity of N-doped $TiO_2$ with $Fe^{3+}$ ions gradually decreased with increased amount of $Fe^{3+}$ ions because a large excess was thought to occupy the active sites on the surface of N-doped $TiO_2$ and functioned as recombination centers between electrons and holes[41].

**Figure 11 (B)** shows the photocatalytic activity of S-doped $TiO_2$ photocatalysts with $Fe^{3+}$ ions. The change in activity of S-doped $TiO_2$ powders with the amount of $Fe^{3+}$ ions was similar to that of N-doped $TiO_2$ with $Fe^{3+}$ ions. S-doped $TiO_2$ with 0.90 wt% $Fe^{3+}$ ions showed the highest photocatalytic activity for oxidation of 2-propanol. The quantum efficiency for the reaction was estimated at 2.1%. The optimum amount of $Fe^{3+}$ cations was slightly different. These results indicated that the doping atoms, and the density of defects located on the surface of the doped $TiO_2$ particles, are important factors to determine the optimum amount of $Fe^{3+}$ ions.

**Figure 12** shows the rate of decomposition of 2-propanol on S-doped $TiO_2$ with and without $Fe^{3+}$ ions as a function of the cutoff wavelengths of the glass filters irradiated with a Xe lamp. Although the absorption spectra of S-doped $TiO_2$ with and without $Fe^{3+}$ ions were very similar, the photocatalytic activity of S-doped

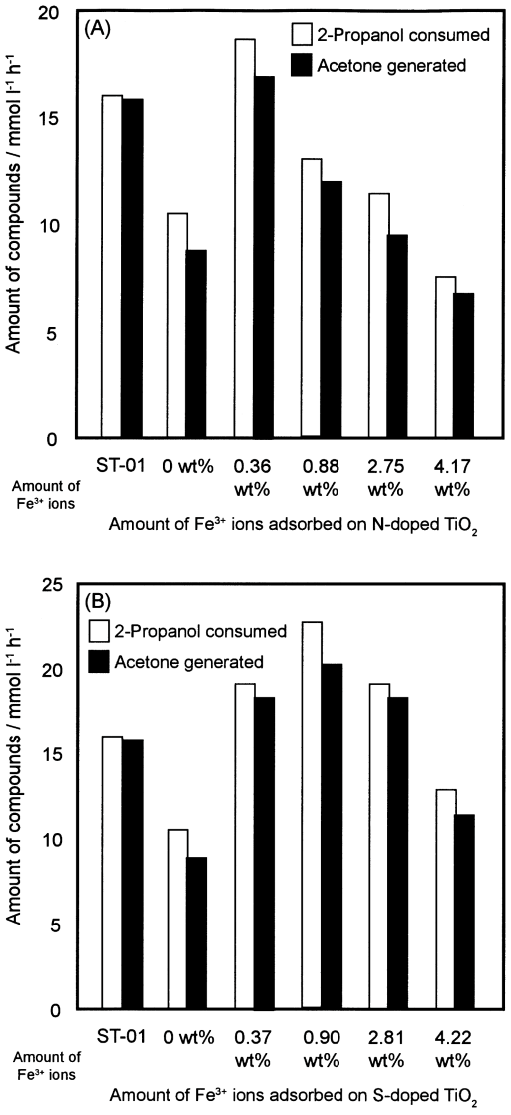


(A) N-doped $TiO_2$, (B) S-doped $TiO_2$.

Fig. 11 Photocatalytic Activities of Doped $TiO_2$ with Adsorbed $Fe^{3+}$ Ions as Well as ST-01 for Oxidation of 2-Propanol under Photoirradiation at Wavelengths Longer than 350 nm

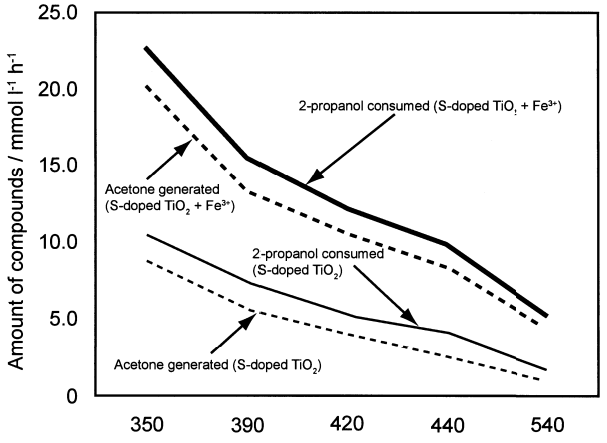


The amount of $Fe^{3+}$ ion is 0.90 wt%.

Fig. 12 Photocatalytic Activities of S-doped $TiO_2$ Powders with and without Adsorbed $Fe^{3+}$ Ions for Oxidation of 2-Propanol as a Function of the Cutoff Wavelength of Incident Light

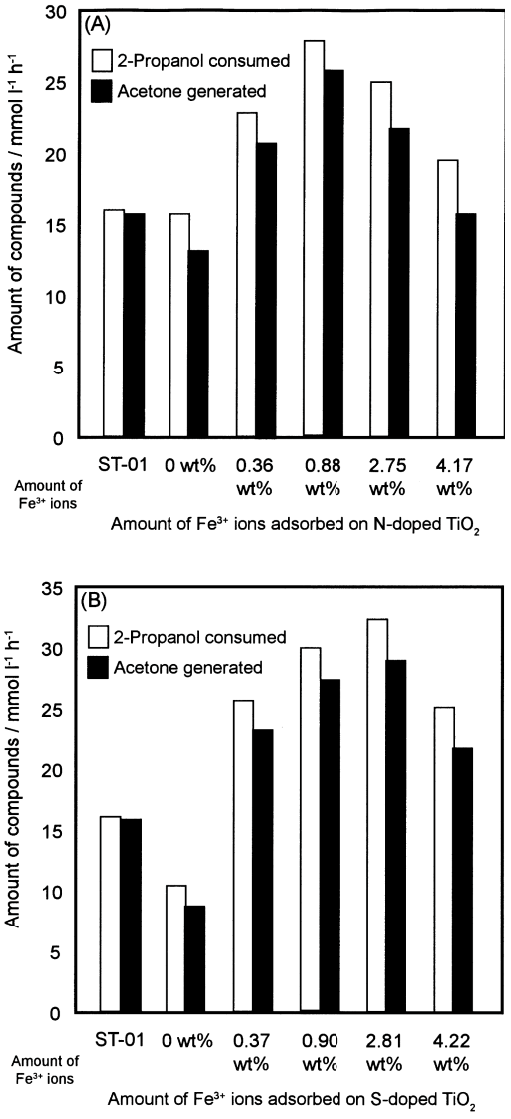


(A) N-doped $TiO_2$, (B) S-doped $TiO_2$.

Fig. 13 Photocatalytic Activities of Doped $TiO_2$ with Adsorbed $Fe^{3+}$ Ions Treated with $NaBH_4$ and Air Oxidation as Well as ST-01 for Oxidation of 2-Propanol under Photoirradiation at Wavelengths Longer than 350 nm

$TiO_2$ with $Fe^{3+}$ cations was about 2.5 times higher under a wide range of irradiation wavelengths. Similar improvement in the photocatalytic activity of N-doped $TiO_2$ with $Fe^{3+}$ cations was also observed (data not shown). These results suggest that the improvement in photocatalytic activities of S- or N-doped $TiO_2$ with adsorbed $Fe^{3+}$ ions under a wide range of irradiation wavelengths including UV and visible light originates from electron trapping by $Fe^{3+}$ compounds on S- or N-doped $TiO_2$ particles.

### 3. 9. 2. Photocatalytic Activities of S- or N-doped $TiO_2$ Photocatalysts with Adsorbed $Fe^{3+}$ Ions Treated with $NaBH_4$ and Air Oxidation (redox treatment)

The photocatalytic activities of N-doped $TiO_2$ with $Fe^{3+}$ ions for oxidation of 2-propanol were investigated before and after $NaBH_4$ and air oxidation. The photocatalytic activity was higher after redox treatment with 0.88 wt% $Fe^{3+}$ ions adsorbed on the surface of N-doped $TiO_2$ as shown in **Fig. 13 (A)**. The optimum amount of $Fe^{3+}$ on N-doped $TiO_2$ for oxidation of 2-propanol after treatment with $NaBH_4$ and air oxidation was slightly higher than that without $NaBH_4$ treatment. S-doped $TiO_2$ with $Fe^{3+}$ ions treated with $NaBH_4$ and air oxidation showed similar tendencies as shown in **Fig. 13 (B)**. The maximum quantum efficiency of S-doped $TiO_2$ with $Fe^{3+}$ ions (2.81 wt%) after treatment with $NaBH_4$ was estimated at 3.0%.

As described above, the crystal structure of Fe compounds on S- or N-doped $TiO_2$ changed from $\gamma$-$Fe_2O_3$ to $\gamma$-FeO(OH) after treatment with $NaBH_4$ and air oxidation. Although the main factor responsible for improving the photocatalytic activity of S- or N-doped $TiO_2$ with $Fe^{3+}$ ions after treatment with $NaBH_4$ and air oxidation is not clear yet, the change in crystal structure of the Fe compounds is thought to be an important factor.

## 4. Conclusions

S-doped $TiO_2$ photocatalysts were prepared. The S atoms were mainly tetravalent. The S-doped $TiO_2$ powder, which has relatively high photocatalytic activity under visible light at wavelengths longer than 500 nm, may have a wide range of applications. In particular, hydroxylation of adamantane is interesting from the viewpoint of organic syntheses in connection with green chemistry, because adamantane can be con-

verted to hydroxylated derivatives using molecular oxygen under a wide range of incident wavelengths including UV and visible light.

In addition, S- or N-doped $TiO_2$ with adsorbed $Fe^{3+}$ cations were also prepared. The photocatalytic activity for oxidation of 2-propanol was 2-4 times higher than for S- or N-doped $TiO_2$ without $Fe^{3+}$ ions. Improvement in the photocatalytic activity by $Fe^{3+}$ treatment was observed under a wide range of irradiation wavelengths, including UV light and visible light. $Fe^{3+}$ ions adsorbed on the surface of S- or N-doped $TiO_2$ particles efficiently trapped the photoexcited electrons generated in the photocatalysts, resulting in improvement in charge separation between electrons and holes. In addition, the photocatalytic activities of S- or N-doped $TiO_2$ with adsorbed $Fe^{3+}$ ions increased markedly after treatment with $NaBH_4$ and air oxidation. The change in the crystal structure of Fe compounds on the doped $TiO_2$ photocatalysts is probably important in the improvement of photocatalytic activity.

S- or N-doped $TiO_2$ powder with adsorbed $Fe^{3+}$ ions, which have high photocatalytic activities under a wide range of irradiation wavelengths, may have a wide variety of practical applications. We expect that the catalytic activity will be further improved by optimizing the conditions for preparing the S- or N-doped $TiO_2$ powders with adsorbed $Fe^{3+}$ ions.

**Acknowledgment**

This work was supported by a Grant-in-Aid for Scientific Research on Priority Areas (417) from the Ministry of Education, Culture, Science, and Technology (MEXT), Japan and Nissan Science Foundation.

## References

1) Fujishima, A., Honda, K., *Nature*, **238**, 5551 (1972).
2) Hoffman, M. R., Martin, S. T., Choi, W., Bahnemann, D. W., *Chem. Rev.*, **95**, 69 (1995).
3) Cao, L., Spiess, F., Huang, A., Suib, S. L., Obee, T. N., Hay, S. O., Freihaut, J. D., *J. Phys. Chem.*, **103**, 2912 (1999).
4) Wolfrum, E. J., Huang, J., Blake, D. M., Maness, P. C., Huang, Z., Fiest, J., Jacoby, W. A., *Environ. Sci. Technol.*, **36**, 3412 (2002).
5) Theurich, J., Bahnemann, D. W., Vogel, R., Dhamed, F. E., Alhakimi, G., Rajab, I., *Res. Chem. Intermed.*, **23**, 247 (1997).
6) Yanagida, S., Ishimaru, Y., Miyake, Y., Shiragami, T., Pac, C., Hashimoto, K., Sakata, T., *J. Phys. Chem.*, **93**, 2576 (1989).
7) Ohtani, B., Kawaguchi, J., Kozawa, M., Nishimoto, S., Inui, T., *J. Chem. Soc., Faraday Trans.*, **91**, 1103 (1995).
8) Ohno, T., Kigoshi, T., Nakabeya, K., Matsumura, M., *Chem. Lett.*, **877** (1998).
9) Ohno, T., Nakabeya, K., Matsumura, M., *J. Catal.*, **176**, 76 (1998).
10) Soana, F., Sturini, M., Cermenati, L., Albini, A., *J. Chem. Soc., Perkin Trans.*, **2**, 699 (2000).
11) Mattews, R. W., *J. Chem. Soc., Faraday Trans. 1*, **80**, 457 (1984).
12) Fujihira, M., Satoh, Y., Osa, T., *Nature*, **293**, 206 (1981).
13) Dusi, M., Muller, C. A., Mallat, T., Baiker, A., *Chem. Commun.*, 197 (1999).
14) Ohno, T., Tanigawa, F., Fujihara, K., Izumi, S., Matsumura, M., *J. Photochem. Photobiol., A*, **127**, 107 (1999).
15) Anpo, M., *Catal. Surv. Jpn.*, **1**, 169 (1997).
16) Ghosh, A. K., Maruska, H. P., *J. Electrochem. Soc.*, **124**, 1516 (1977).
17) Choi, W., Termin, A., Hoffmann, M. R., *J. Phys. Chem.*, **98**, 13669 (1994).
18) Breckenridge, R. G., Hosler, W. R., *Phys. Rev.*, **91**, 793 (1953).
19) Cronemeyer, D. C., *Phys. Rev.*, **113**, 1222 (1957).
20) Ohno, T., Masaki, Y., Hirayama, S., Matsumura, M., *J. Catal.*, **204**, 163 (2001).
21) Ikeda, S., Abe, C., Torimoto, T., Ohtani, B., *Electrochemistry*, **70**, 442 (2002).
22) Asahi, R., Morikawa, T., Ohwaki, T., Aoki, A., Taga, Y., *Science*, **293**, 269 (2001).
23) Sakatani, Y., Okusato, K., Koike, H., Ando, H., *Photocatalysis*, **4**, 51 (2001).
24) Ihara, T., Ando, M., Sugihara, S., *Photocatalysis*, **5**, 19 (2001).
25) Umebayashi, T., Yamaki, T., Ito, H., Asai, K., *Appl. Phys. Lett.*, **81**, 454 (2002).
26) Irie, H., Watanabe, Y., Hashimoto, K., *Chem. Lett.*, **32**, 772 (2003).
27) Sakthivel, S., Kisch, H., *Angew. Chem., Int. Ed. Engl.*, **42**, 4908 (2003).
28) Ohno, T., Mitsui, T., Matsumura, M., *Chem. Lett.*, **32**, 364 (2003).
29) Ohno, T., Akiyoshi, M., Umebayashi, T., Asai, K., Mitsui, T., Matsumura, M., *Appl. Catal. A: General*, **265**, 115 (2004).
30) Ohno, T., Tsubota, T., Nishijima, K., Miyamoto, Z., *Chem. Lett.*, **33**, 750 (2004).
31) Ohno, T., Tsubota, T., Toyofuku, M., Inaba, R., *Catal. Lett.*, **98**, 255 (2004).
32) Blaha, P., Schwarz, K., Sorantin, P., Trickey, S. B., *Comput. Phys. Commun.*, **59**, 399 (1990).
33) Perdew, J. P., Burke, K., Ernzerhof, M., *Phys. Rev. Lett.*, **77**, 3865 (1996).
34) Kohn, W., Sham, L. J., *Phys. Rev.*, **140**, 1133 (1965).
35) Umebayashi, T., Yamaki, T., Yamamoto, S., Miyashita, A., Tanaka, S., Sumita, T., Asai, K., *J. Appl. Phys.*, **93**, 5156 (2003).
36) Umebayashi, T., Yamaki, T., Itoh, H., Asai, K., *J. Phys. Chem. Solids*, **63**, 1909 (2002).
37) Nosaka, Y., Matsushita, M., Nishino, J., Nosaka, AY., *Science and Technology of Advanced Materials*, **6**, 1468 (2005).
38) Khaleel, A. A., *Chem. Dur. J.*, **10**, 925 (2004).
39) Stanjek, H., *Clay Minerals*, **37**, 629 (2002).
40) Nakanishi, T., Iida, H., Osaka, T., *Chem. Lett.*, **32**, 1166 (2003).
41) Fujihara, K., Izumi, S., Ohno, T., Matsumura, M., *J. Photochem. Photobiol., A*, **132**, 99 (2000).

## 要　　旨

### 可視光応答性二酸化チタン光触媒の開発と鉄イオンを用いた高感度化

横野　照尚

九州工業大学工学部物質工学科，804-8550 北九州市戸畑区仙水町1-1

二酸化チタン光触媒は環境浄化用の重要な触媒と考えられているが，その触媒活性は紫外光照射下でしか発現しない。したがって，我々は，太陽光のような広範囲な光を励起光源に利用するために，可視光化で触媒活性を発現する光触媒の開発は重要と考えている。そこで，我々は硫黄カチオンを二酸化チタンのチタンイオンの一部，あるいは窒素アニオンを二酸化チタンの酸素イオンの一部と置換した可視光応答型二酸化チタン光触媒を開発した。これらは，可視光領域に強い吸収を示し，440 nm の可視光照射下で2-プロパノールやアダマンタンの部分酸化反応を効率よく進行させる。XPS 測定により硫黄と窒素の酸化状態を測定したところ，ドープされた硫黄の酸化数は主に $S^{4+}$ であり，窒素の酸化数は $N^{3-}$ であった。さらに，硫黄と窒素をドープした可視光応答型二酸化チタンの粒子表面に鉄イオンを吸着処理することで，触媒活性が大きく向上した。このときの最適な鉄イオン吸着量は，硫黄ドープ二酸化チタンの場合で0.9 wt%，窒素ドープに酸化チタンの場合で0.36 wt% であった。これら鉄吸着処理を行った硫黄および窒素ドープ二酸化チタンは，水素化ホウ素ナトリウムにより吸着処理した鉄イオンの還元，空気再酸化により，さらに活性が向上することが明らかになった。

このときの最適な鉄イオン吸着量は，硫黄ドープ二酸化チタンの場合で2.81 wt%，窒素ドープに酸化チタンの場合で0.88 wt% であった。

……